Available online at www.sciencedirect.com
SCIENCE DIRECT
Polymer 46 (2005) 6154–6162
polymer
www.elsevier.com/locate/polymer

Collapsed chains as models for filler particles in a polymer melt

Heng Lin, Fatih Erguney*, Wayne L. Mattice

Department of Polymer Science, University of Akron, Akron, OH 44325-3909, USA

Received 7 March 2005; received in revised form 12 April 2005; accepted 12 April 2005
Available online 14 June 2005

Abstract

Simulations of dense melts of coarse-grained chains have been modified so that they contain filler particles. Since the filler particles and matrix chains are constructed from the same repeat unit, all of the intermolecular energetic interactions in the system (filler–filler, filler–matrix, matrix–matrix) are identical. The collapse of individual chains to form filler particles is achieved by a simple modification in the strength of the minimum in the Lennard–Jones potential governing pair-wise intramolecular interactions within a filler particle. Even when completely collapsed, the filler particles retain mobility in their internal degrees of freedom. Their centers of mass are also mobile. The filler particles can be collapsed completely to dense, impenetrable objects, but they can also be collapsed incompletely to produce permeable filler particles.

There is no evidence for spontaneous aggregation of impermeable filler particles, but sufficiently permeable filler particles can aggregate. The parameters used in the simulations insure that the aggregation cannot be energetically driven. Matrix chains that fill space within a permeable filler particle have severe restrictions placed on their available conformations. The reduction in the conformational entropy of the matrix chains can be alleviated if the permeable filler particles interpenetrate, or aggregate. Then fewer matrix chains must enter the permeable filler particles in order to maintain the density of the system. The simulation detects no aggregation of impermeable filler particles because it is not necessary for matrix chains to enter completely collapsed particles.

Keywords: Composites; Filled polymers; Filler particles

1. Introduction

The importance of filled polymers has prompted numerous studies that characterize the dramatic effects of the filler particles on the physical properties of the system. Simulations of filled polymers have been performed using molecular dynamics (for example, Starr et al. [1] and Brown et al. [2]) and Monte Carlo (for example, Mark and co-workers [3,4] and Vacatello [5,6]) techniques. Often the filler particle and the matrix chains are not represented in atomistic detail. The filler particle may be represented by a simple impenetrable object, such as a sphere [3–6] or icosahedron [1], with an undefined internal composition. Matrix chains are often represented by a bead-spring model [1,2,5,6], and therefore cannot unambiguously be identified with a specific polymer. Sometimes the chain (but not the particle) is represented with sufficient detail so that it can be identified with a real polymer, such as polydimethylsiloxane [3] or polyethylene [4], and sometime the particle (but not the chain) can be identified with a real material, such as silica [2]. Since the qualitative results can depend dramatically on the method and/or model employed [5], it seems worthwhile to develop simulation methods in which both the filler particle and matrix chains can be unambiguously identified with specific real materials. Here we describe one approach by which this goal can be achieved.

The method by which our nanoparticles are created in the simulation is based on a well-known phenomenon seen with polymers in dilute solution. The collapse of individual polymer chains, sometimes described as the coil-to-globule transition, has been studied extensively in dilute solution, using experiment [7–12], theory [13], and simulation [14]. A change in solvent power from better than a Θ solvent to new conditions that are worse than a Θ solvent will induce the transition. This change in solvent power is often induced by a change in the temperature, T, as illustrated by polystyrene in cyclohexane [7,8], poly(*N*-isopropyl-

* Corresponding author. Tel.: +1 330 283 7089.
E-mail address: erguney@gmail.com (F. Erguney).

0032-3861/$ - see front matter © 2005 Elsevier Ltd. All rights reserved.
doi:10.1016/j.polymer.2005.04.103

acrylamide) in water [9,10], and poly(methyl methacrylate) in isoamyl acetate [11] or acetonitrile [12]. Experimental characterization of the purely intramolecular transition requires great care to properly take account of the influence of the polydispersity of real samples [8] and avoid the influence of intermolecular interactions that lead to aggregation [7]. The influence of aggregation is minimized by the experimental study of extremely dilute solutions of samples of very high molecular weight, M. Although measurements show that the mean square radius of gyration, $\langle s^2 \rangle$, approaches the $M^{2/3}$ dependence expected for completely collapsed chains, the collapsed chains remain permeable to solvent [8].

With the assistance of intramolecular crosslinks, it is possible to also study systems in which collapsed chains coexist with uncollapsed chains in the Θ environment provided by chemically similar, but uncrosslinked, chains. This system can be realized in the laboratory by the introduction of an extensively intramolecularly crosslinked polystyrene nanoparticle into a system composed of linear polystyrene chains [15]. The constraints imposed by the intramolecular crosslinks do not allow the nanoparticle to recover the unperturbed, or Θ, dimensions expected for a chain in an uncrosslinked melt.

A melt composed exclusively of chains that are all constructed from the same repeat unit, but under constraints that enforce a collapse on some of the chains, provides an entrée to potentially illuminating studies concerning the fundamental interactions in filled polymers. Any modification of the behavior of the uncollapsed chains cannot be due to a special energetic interaction between the matrix chains and filler particles, because the 'particles' and free chains are constructed from the same repeat unit. Simulations of this system will allow a clean separation of effects arising from the physical space occupied by the filler particle, as opposed to any effects arising from the energetic interaction of the filler particle with the free chains. Furthermore, since the degree of collapse of such filler particles can be carefully controlled in a simulation, one can monitor how the special characteristics of a filled system are produced as specified chains in the system progress gradually through the sequence unperturbed free chains → partially collapsed, permeable filler particles → completely collapsed, impermeable filler particles. Depending on the physical property of the system that is monitored, the change in the property might be monotonic, sigmoid, or perhaps of more complex character, as the collapse of the 'filler' becomes more complete. Of course, the filler particle should not be collapsed to an unphysical density that is higher than the value expected for the melt. This requirement is easily met.

We describe here the preparation of one-component filled systems in which all of the chains in the melts are coarse-grained versions of either polyethylene (PE) or polyoxyethylene (POE), but with a subset of the chains collapsed to varying degrees. The collapse is entirely intramolecular in origin. All pair wise intermolecular interactions between beads are independent of whether the beads reside on collapsed or uncollapsed chains.

2. Simulation method

All of the Monte Carlo (MC) simulations are performed using a bridging method [16] that allows reversible description of the system by coarse-grained chains on a sparsely occupied high coordination lattice or by atomistically detailed chains at bulk density in continuous space [17]. Each coarse-grained bead represents two consecutive chain atoms and their pendant hydrogen atoms. The high coordination lattice, with $10i^2+2$ sites in shell i, has a step length of 0.250 nm for PE [18] and 0.239 nm for POE [19]. Bulk density, ρ, for PE melts and POE melts at the T of the simulations (453 K for PE, 373 K for POE) is obtained by occupancy of 18% [20] and 20% [19], respectively, of the sites on the high-coordination lattice.

The short-range intramolecular interactions are controlled by the first- and second-order interactions in rotational isomeric state (RIS) models for PE [21] and POE [22]. These RIS models are mapped onto the coarse-grained description of the chains on the high coordination lattice [23]. Longer range intramolecular interactions, and all intermolecular interactions, are controlled by a discretized Lennard–Jones (LJ) potential energy function. In addition to disallowing double occupancy of any site, this function has a set of shell energies, denoted u_i for shell i, that reproduce the second virial coefficient specified by an input continuous LJ potential of the form in Eq. (1) [20].

$$U_{\mathrm{LJ}} = 4\varepsilon\left[\left(\frac{\sigma}{r}\right)^{12} - \left(\frac{\sigma}{r}\right)^{6}\right] \tag{1}$$

The input LJ potentials use $\sigma = 0.44$ nm and $\varepsilon/k_{\mathrm{B}} = 185$ K for PE, and $\sigma = 0.376$ nm and $\varepsilon/k_{\mathrm{B}} = 154$ K for POE. At the temperatures of the simulations, these LJ potentials specify $u_1 = 14.426$, $u_2 = 0.558$, and $u_3 = -0.626$ kJ/mol for PE, and $u_1 = 8.113$, $u_2 = -0.213$, and $u_3 = -0.339$ kJ/mol for POE. The u_i for $i > 3$, which are negative and smaller in absolute value than u_3, were ignored in the present simulations [19,20].

For those chains that are to collapse to become filler particles, u_3 is separated into two terms, denoted $u_{3,\ \mathrm{inter}}$ and $u_{3,\ \mathrm{intra}}$, in the manner sketched in Fig. 1. The $u_{3,\ \mathrm{intra}}$ is used for the long-range intramolecular interactions (intramolecular interactions that were not treated explicitly with the RIS model) within this particular collapsed chain, and $u_{3,\ \mathrm{inter}}$ is used for the long-range intermolecular interactions between a bead on the collapsed chain and a bead on any other chain, independent of whether that other chain is also collapsed or is instead an unperturbed matrix chain. Since the value of $u_{3,\ \mathrm{inter}}$ remains the same as the value of u_3 specified in the previous paragraph, the discretized LJ

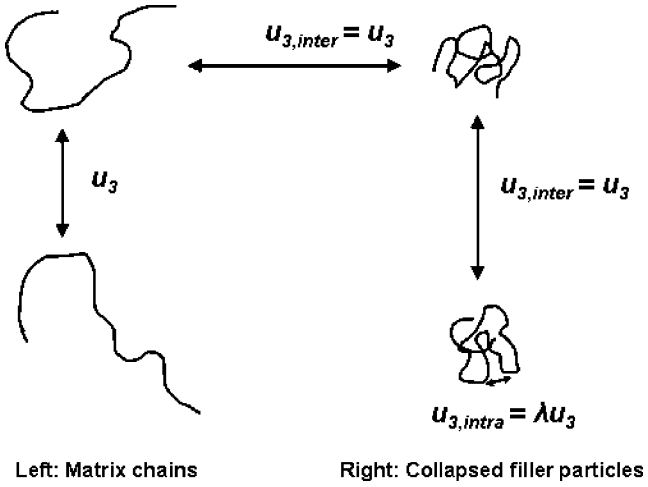

Fig. 1. Sketch showing the usage of $u_{3,\ inter} = u_3$ and $u_{3,\ intra}$.

potential for all intermolecular interactions is unaffected by the formation of collapsed chains. However, pairs of beads within a particular collapsed chain are subject to their own special value of u_3, with the strength of this interaction controlled by λ.

$$u_{3,\ intra} = \lambda u_{3,\ inter} \tag{2}$$

When $\lambda > 1$, there is an enhancement of the attraction between two beads from the collapsed chain when they are separated by a distance that produces the most negative energies in the discretized LJ potential. This extra intramolecular attraction causes a reduction in $\langle s^2 \rangle$ for the collapsed chain. If λ is made large enough, the value of $\langle s^2 \rangle$ will approach $(3/5)(3\nu M/4\pi N_A)^{2/3}$, which is the value expected for a uniform sphere with the mass (M/N_A) and partial specific volume $(\nu = 1/\rho)$ of the collapsed chain. The collapse is a continuous process, since λ is a continuous variable. The collapse is also purely of intramolecular origin, since $u_{3,\ inter}$ retains the value expected for uncollapsed chains in the melt. The energetically driven aggregation of collapsed chains, which is a formidable problem in the experimental study of the coil-to-globule transition in dilute solution, is shut down completely in the present simulations by the assignment $u_{3,\ inter} = u_3$.

The Metropolis MC simulation [24] used single bead moves [17] and pivot moves for 2–6 beads [25]. If X and Y denote chain atoms that are (X) or are not (Y) retained in the coarse-grained description, there are rare conformations of the atomistically detailed sub chain X–Y–X–Y–X that avoid placing any two X's on the same site on the high-coordination lattice, but nevertheless place both Y's on the same site on the underlying diamond lattice. These rare conformations of the coarse-grained chain, which have been termed 'collapses' [17,23], were specifically disallowed in the present simulations. On average, each bead is tried once for a single bead move, and once for a pivot move, during a single MC step (MCS).

3. Collapse from equilibrated melts

The simulation of the filled systems begins with equilibrated melts of PE or POE, i.e. systems equilibrated using $\lambda = 1$. The equilibration and characterization of these melts has been described previously [17,19]. At the beginning of the simulations of the filled systems, a randomly chosen subset of the parent chains in the equilibrated melt was subjected to the $u_{3,\ intra}$ specified by Eq. (2), using $\lambda > 1$. The concentration of the filler particles, x_{filler}, expressed as a volume (or mass) fraction, is the fraction of the beads in the system that belongs to chains subject to $\lambda > 1$. The remainder of the chains are uncollapsed, with $\lambda = 1$. The rate at which the filler chains collapse is revealed by monitoring the values of their mean square radii of gyration, $\langle s^2 \rangle_{filler}$, as a function of the number of MCS after the value of λ is changed from 1 to a number larger than 1.

Fig. 2 depicts $\langle s^2 \rangle_{filler}$ for POE melts in which all of the 43 parent chains are represented by 52 beads. The simulation commences with an equilibrated melt where the chains have a time-averaged mean square radius of gyration of 1.5 nm^2. The change in the numerical assignment for λ from 1 to 2.5 occurs at 0 MCS. When the fluctuations are considered, the limiting values of $\langle s^2 \rangle_{filler}$ are nearly independent of x_{filler}. However, the rate at which the collapse is achieved depends strongly on x_{filler}. The collapse is completed in about 10^5 MCS if $x_{filler} = 0.05$, but an order of magnitude more MCS is required if $x_{filler} = 0.60$.

The dependence of the rate of collapse on x_{filler} is seen also in a system with larger particles constructed from PE, as shown in Fig. 3. In both Figs. 2 and 3, the slowing down of the collapse is evident when $x_{filler} = 0.60$. There are some important differences in the two systems. The collapse is completed quickly (within 10^5–10^6 MCS, depending on x_{filler}) for the POE system, but at least 10^7 MCS are required for the collapse of the PE chains. This difference arises because the individual PE particles are over three times larger than the POE particles (174 and 52 beads, respectively), PE is a stiffer chain than POE, and perhaps also because the PE filler particles become more strongly collapsed than the POE filler particles, as will be documented in Section 4. The slowing down of the collapse at $x_{filler} = 0.60$ might have contributions from two sources. First, the rate at which a chain collapses may depend on whether its neighbors remain uncollapsed, or whether they are also undergoing an intramolecular collapse. Obviously, it becomes more likely that neighboring chains also experience the intramolecular collapse as the values of x_{filler} increases. There might also be an effect from more stringent requirements for the spatial arrangements of the filler particles in the final state as x_{filler} increases. At small values of x_{filler} the filler particles can be independent of one another, but percolation may be achieved when x_{filler} becomes as large as 0.60. The spatial requirements in the

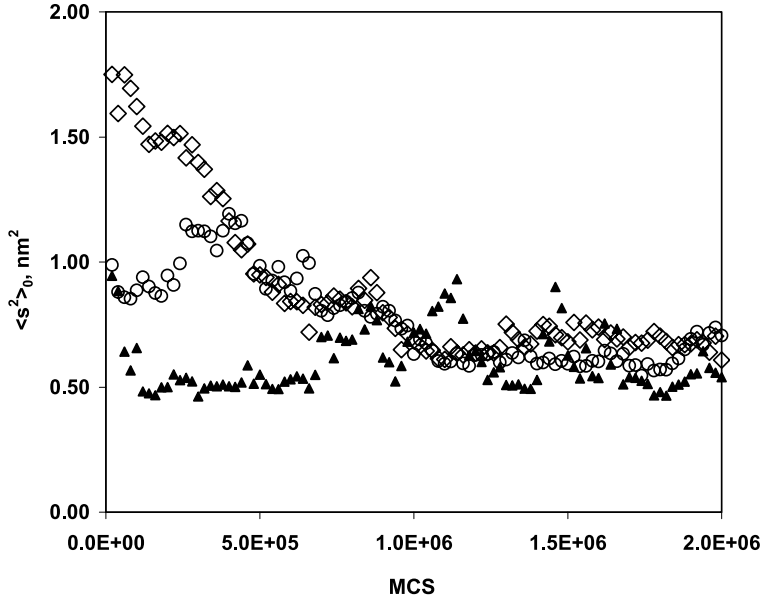

Fig. 2. Collapse of POE filler particles at 373 K when all of the 43 parent chains are represented by 52 beads, $\lambda = 2.5$, and x_{filler} is (▲) 0.05, (○) 0.10, or (◇) 0.60. The value of $\langle s^2 \rangle_0$ is 1.5 nm^2.

percolating system may contribute to the final stages of the slowing down of the collapse at $x_{\text{filler}} = 0.60$.

4. Properties of the collapsed filler particles

4.1. Extent of the collapse

There are differences in the magnitudes of the fluctuations in $\langle s^2 \rangle_{\text{filler}}$ at 1 to 2 million MCS in Fig. 2 and near 10^7 MCS for the smaller three of the four x_{filler} in Fig. 3. These differences suggest larger fluctuations in the POE system. Interpretation of this result is facilitated by specification of the extent of collapse that is achieved in the two simulations. A convenient measure of the extent of the collapse is provided by the dimensionless parameter defined in Eq. (3) using the mean square unperturbed radius of gyration of the chains in the melt equilibrated with $\lambda = 1$, denoted $\langle s^2 \rangle_0$, the instantaneous mean square radius of gyration of the collapsed chains, denoted $\langle s^2 \rangle_{\text{filler}}$, and the anticipated squared radius of gyration for the dense sphere with mass M/N_A and partial specific volume v.

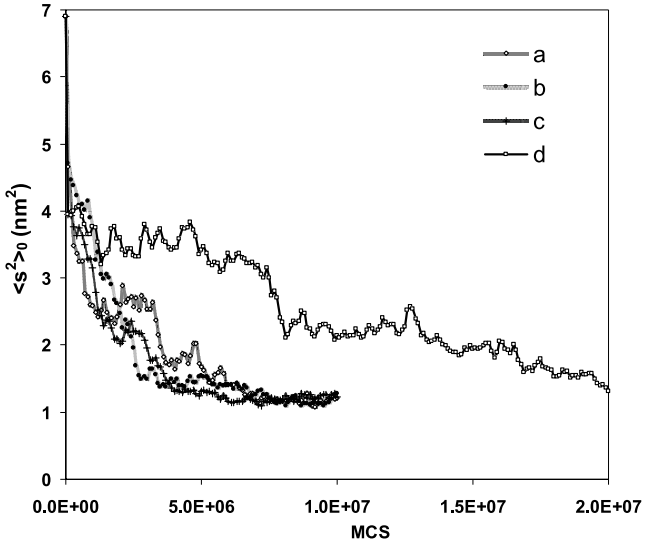

Fig. 3. Collapse of PE filler particles of 174 beads at 453 K. The uncollapsed parent chains are each represented by 58 beads. The value of λ is 2, and x_{filler} is (a) 0.24, (b) 0.36, (c) 0.48 or (d) 0.60. The value of $\langle s^2 \rangle_0$ for the filler particles before collapse is 6.9 nm^2.

$$c = \frac{\langle s^2 \rangle_0^{3/2} - \langle s^2 \rangle_{\text{filler}}^{3/2}}{\langle s^2 \rangle_0^{3/2} - \left(\frac{3}{5}\right)^{3/2} \left(\frac{3vM}{4\pi N_A}\right)} \tag{3}$$

As defined, c measures the fractional change in the volumes specified by the various radii of gyration, using limits of $c = 0$ when there is no collapse whatsoever, and $c = 1$ upon collapse to the dense impermeable sphere with mass M/N_A and partial specific volume v.

The average limiting values of c are about 0.80 ± 0.06 for the POE filler particles in Fig. 2, but c achieves values of 1.00 ± 0.02 for the larger filler particles in Fig. 3. The values of λ employed in the simulations produce a more complete collapse of the PE filler particles than the POE filler particles. The PE filler particles are dense and impermeable, with relatively small fluctuations in their sizes. In contrast, the POE filler particles are less dense (and therefore permeable), and experience larger fluctuations in size. These differences should not be attributed to any special characteristics of PE or POE, because a suitable increase in the value of λ for POE can produce POE filler particles with c much closer to 1, as shown in Fig. 4.

The value of λ required to produce a particular value of c

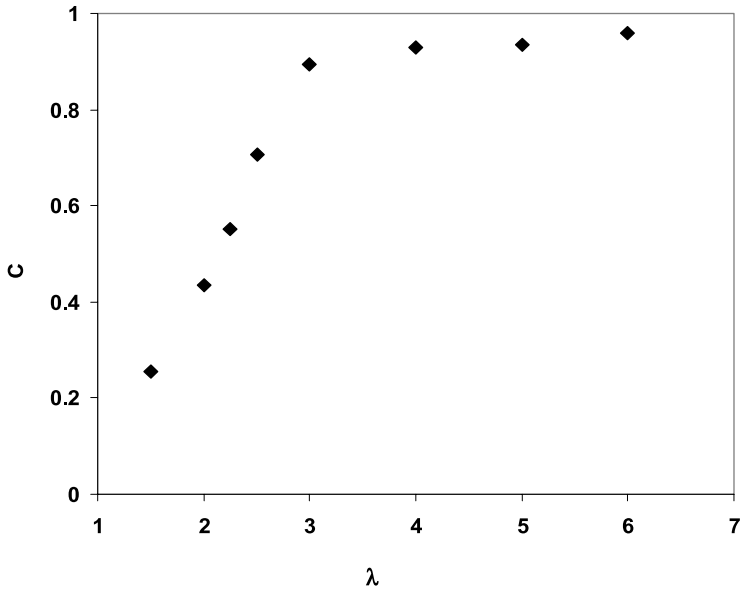

Fig. 4. Values of c after equilibration of a POE system at 373 K when the filler particles of 52 beads use various values of λ. The values of x_{filler} are in the range 0.05–0.30.

depends on M of the filler particles, as shown in Fig. 5 for PE filler particles. Smaller values of λ will suffice at larger M. This behavior in the simulation is consistent with the experimental observation in dilute solution that, for a specified undercooling, a greater collapse is seen with chains of higher M.

4.2. Mobility of the collapsed filler particles

If the same attempt rate is used for moves of all beads in the system, the filler particles can remain mobile even when they are collapsed to the extent where c is very close to one. The internal mobility can be monitored using the normalized autocorrelation function for the end-to-end vector, $\langle \mathbf{r}(t+t_0)\cdot\mathbf{r}(t_0)\rangle/\langle r^2\rangle$, after completion of the collapse. Examples are depicted in Fig. 6 for two PE systems, showing separately the autocorrelation functions for the impermeable particles and the uncollapsed matrix chains. The relaxation times for the impermeable filler particles become longer as the particles become larger, as expected. The relaxation times for matrix chains of 58 beads are not much different in systems with $x_{\text{filler}}=0.28\pm0.04$ and individual fillers that are either 0.26 or 3.00 times as massive as a matrix chain.

The translational motion of the filler particles is

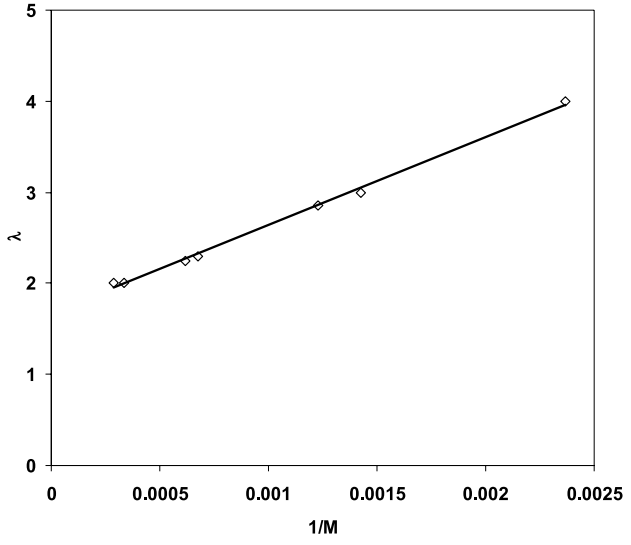

Fig. 5. Minimum values of λ required to achieve $c=1.00\pm0.02$ for PE filler particles at 453 K.

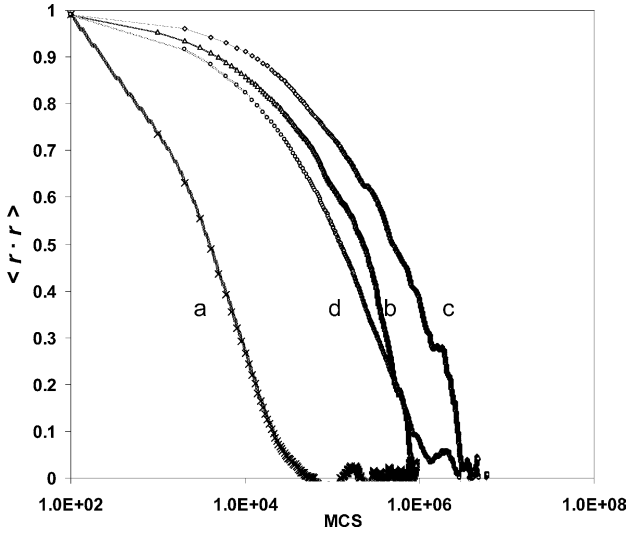

Fig. 6. Normalized autocorrelation functions for $\mathbf{r}$ in impermeable PE filler particles collapsed to $c=1.00\pm0.02$ at 453 K. The uncollapsed matrix chains are represented by 58 beads. (a) Filler particles of 15 beads and (b) matrix chains in the system with $x_{\text{filler}}=0.24$. (c) Filler particles of 174 beads and (d) matrix chains in the system with $x_{\text{filler}}=0.32$.

monitored with the mean square displacement of their centers of mass, $\langle[R_{cm}(t+t_0)-R_{cm}(t_0)]^2\rangle$. Fig. 7 depicts these displacements for the impermeable PE particles that were the subject of Fig. 6. Completely collapsed particles can experience significant translation over the time period of a simulation. The filler particles do not remain static at arbitrarily chosen initial positions. During a simulation of several million MCS, they can diffuse over distances comparable with the linear dimension of the periodic box.

Of course, the filler particles in the simulation can be rendered immobile by not attempting a move for any of their beads. Also, they can be caused to move more rapidly, relative to the matrix chains, simply by attempting more moves for filler particles than for matrix chains. The results in Figs. 6 and 7 were obtained using the same attempt rates for all beads, independent of the chain in which they occur.

4.3. Preferred distributions of the filler particles

If only a single parent chain is collapsed to a filler particle, the pattern formed by this filler particle and its images is determined completely by the dimensions of the periodic box, and is independent of any translational motion of the single parent particle. However, when multiple parent chains are collapsed, they can sample variously relationships with respect to one another during the course of the simulation. They have the option of adopting an ordered arrangement, or instead sampling the wide variety of configurations consistent with a random array of particles. Since in Section 4.2 demonstrated that the centers of mass of the particles can translate over distances comparable with the dimension of a periodic box, it becomes pertinent to inquire how they distribute themselves in the present

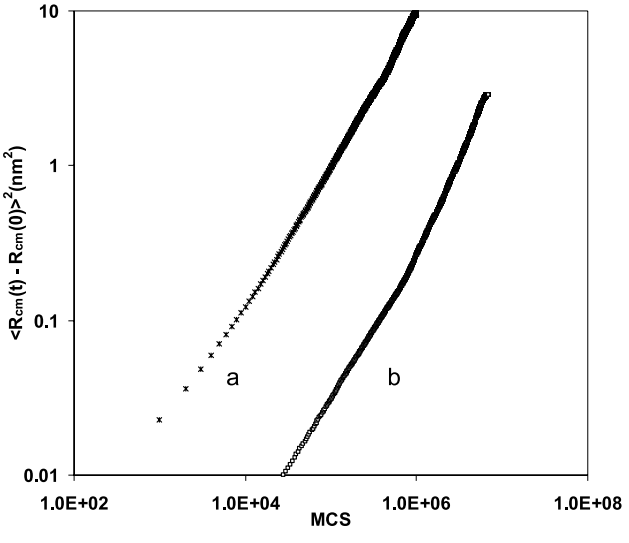

Fig. 7. Mean square displacements of the center of mass for impermeable PE filler particles collapsed to $c=1.00\pm0.02$ at 453 K. The uncollapsed matrix chains are represented by 58 beads. (a) $x_{filler}=0.24$ and filler particles represented by 15 beads. (b) $x_{filler}=0.32$ and filler particles represented by 174 beads.

simulations, when the same attempt rate is used for moves on all beads in the system. Since exactly the same discretized LJ potential describes all of the intermolecular interactions in the system, there can be no tendency for organization of the particles due to special intermolecular energetic effects. Nevertheless, it is still worthwhile to investigate the spontaneous distributions assumed by the filler particles, because even hard spheres adopt ordered patterns at sufficiently high packing densities.

Intermolecular pair correlation functions (PCF's) have a long history of use in the search for and characterization of intermolecular structure. In a perfectly crystalline system, the PCF's consist of discrete spikes that can be observed even at large distances. This type of intermolecular PCF would be obtained for the present system if it was evaluated using the center of mass of the particles, and only one of the parent chains was collapsed. The locations of the discrete peaks would be determined completely by the size and shape of the periodic box. If multiple parent chains are used, the set of discrete peaks expected from the size and shape of the periodic box is supplemented by additional information that depends on the relationship between the positions of the collapsed chains within a periodic box. It is that information that we seek. When the intermolecular PCF is evaluated at distances that do not exceed half of the length of a side of the periodic box, is the PCF predominantly flat, with values close to one (as expected for a random array of objects), or are there pronounced maxima and minima (expected for a nonrandom arrangement)?

In principal, a very interesting intermolecular PCF would use the centers of mass of the individual nanoparticles. This intermolecular PCF is pertinent to the issue of whether the centers-of-mass are distributed randomly in the periodic box, or instead prefer some nonrandom arrangement. Unfortunately, that type of intermolecular PCF is not easily extracted from our simulations with the desired accuracy, due to the small number of individual parent nanoparticles (2–22 in the simulations reported here), and the length of time required to completely decorrelate one replica with another (Fig. 7). The number of independent observations is simply too small to generate intermolecular PCF's with a sufficiently small noise level, if the evaluation is based on the centers of mass of the nanoparticles.

The number of observations increases strongly if the intermolecular PCF's use all of the beads in the nanoparticles, some of the beads are near the center of mass of each nanoparticle, but a larger number are likely to be near the periphery. This type of PCF will retain information about the arrangements of the centers of mass, but now modified (perhaps strongly) by the potential interaction of the periphery of one nanoparticle with the periphery of another. Two limiting cases can be defined. If the arrangements of the nanoparticles is as random as possible, the intermolecular PCF will have very small values at small r (because one nanoparticles tends to exclude any other from the same position), will approach 1

in the limit as $r \to \infty$, and will show a weak (perhaps very weak) maximum at intermediate r, to fulfill the requirement that the integral of PCF—1 over all space must be zero. Examples of intermolecular PCF's, based on all of the beads in the nanoparticles, that fulfill these requirements can be observed in the simulations.

Fig. 8 depicts intermolecular pair correlation functions for PE systems in which the Fig. 8 depicts intermolecular pair correlation functions for PE systems in which the matrix chains are represented by 58 beads and the impermeable filler particles (collapsed to $c = 1.00 \pm 0.02$) are represented by 174 beads. Curves *a* and *c* present the intermolecular pair correlation functions calculated for filler particle–filler particle interactions at two concentrations, $x_{\text{filler}} = 0.60$ and 0.24, respectively, while curves *b* and *d* represent the intermolecular pair correlation functions for matrix chains–matrix chain interactions in the same two systems. The matrix–matrix correlation functions have a weak maximum in the third shell, which is consistent with the 'amorphous halo' present in the intermolecular pair correlation functions for simulations of pure melts of simple polymeric hydrocarbons by this technique [26]. A very different result is obtained with the intermolecular pair correlation functions for beads in the impermeable filler particles. The beads in the collapsed chains that represent the impermeable filler particles have a much stronger tendency to avoid one another than do the beads in uncollapsed chains that represent the matrix chains. The intermolecular pair correlation functions provide no evidence for aggregation of the filler particles, even at x_{filler} as high as 0.60.

There is also no evidence for aggregation of the filler in

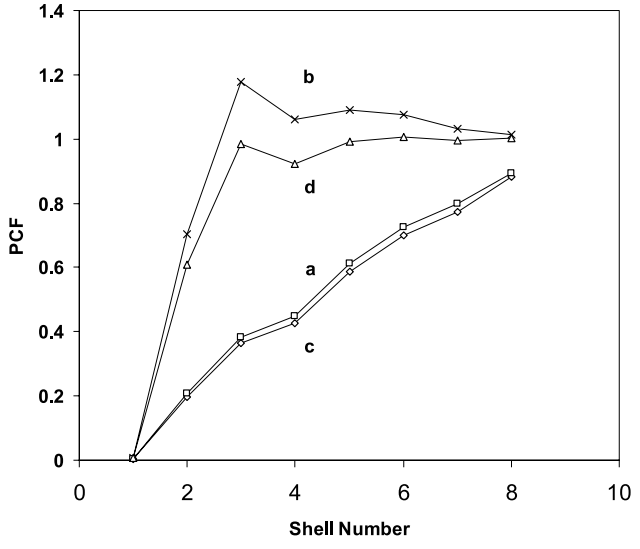

Fig. 8. Intermolecular pair correlation functions for beads in the PE systems at 453 K where the impermeable filler particles, with $c = 1.00 \pm 0.02$, are represented by 174 beads and the matrix chains are represented by 58 beads. For curves (a) and (b), $x_{\text{filler}} = 0.60$, and for curves (c) and (d), $x_{\text{filler}} = 0.24$. The intermolecular pair correlations functions are for filler–filler in curves (a) and (c), and for matrix–matrix in curves (b) and (d).

simulations with slightly permeable POE filler particles of 106 beads that are collapsed to $c = 0.92 \pm 0.01$, as shown in Fig. 9. The particle–particle and matrix–matrix intermolecular pair correlation functions are nearly identical. The situation changes with still smaller POE filler particles (represented by 52 beads) that are even more permeable ($c = 0.85 \pm 0.02$), as shown in Fig. 10. The intermolecular pair correlation function now shows a strong peak when $x_{\text{filler}} = 0.2$, and this peak is much larger than the weak peak observed at the same position, and same value of x_{filler}, when larger filler particles (106 vs. 52 beads) were more strongly collapsed (c of 0.93 vs. c of 0.85), as seen in the comparison of Figs. 9 and 10. A large peak in the intermolecular PCF at the third shell can exist at $x_{\text{filler}} = 0.2$ if the interpenetration at the periphery of penetrable particles is stronger than would be expected from a random arrangement of objects. A tendency for aggregation of the permeable nanoparticles would be a prerequisite for the achievement of that enhanced degree of interpenetration. As x_{filler} increases toward the 'overlap' concentration for the permeable particles, a point will be reached at which the amplitude in the third shell of the intermolecular PCF decreases, because the hypothetical random arrangement will also produce a larger number of third shell intermolecular interactions if the concentration is high enough. Even if the probability for an intermolecular third shell interaction is the same at $x_{\text{filler}} = 0.2$ and 0.5, the intermolecular PCF would be smaller at the higher concentration because the probability for this interaction in the hypothetical disordered state would be larger at the higher value of x_{filler}.

The aggregation of the permeable filler particles at intermediate values of x_{filler} cannot be energetically driven, because all of the pair-wise intermolecular interactions are exactly the same. The aggregation of permeable filler particles, coupled with the absence of evidence for aggregation of the impermeable filler particles, can be rationalized by considering the conformational entropy of the uncollapsed matrix chains. If the filler particles are permeable, some of the matrix chains must occupy space within an unaggregated filler particle in order to maintain the density of the system. The number of conformations available to a matrix chain will be severely restricted if it must fill space within a permeable filler particle. This adverse affect on the conformational entropy of the matrix chains will drive interpenetration, or aggregation, of the permeable filler particles, so that fewer matrix chains must occupy the space within them. Of course, this effect requires that x_{filler} be below the overlap concentration, so that the matrix chains have access to space in the system that is not influenced by the filler particles. The driving force for aggregation is absent if the filler particles are impermeable, which provides an explanation for why the simulation detects spontaneous aggregation of sufficiently permeable filler particles, but no aggregation of impermeable filler particles.

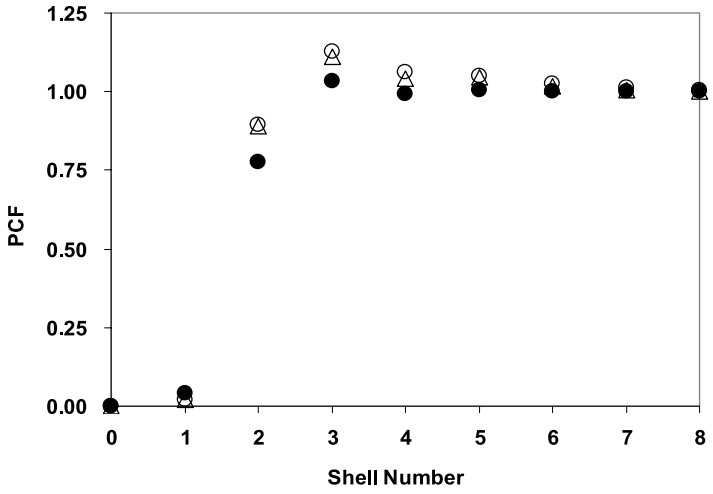

Fig. 9. Intermolecular pair correlation functions for beads in slightly permeable ($c=0.92\pm0.01$) POE filler particles at 373 K and values of x_{filler} of (△) 0.19 and (○) 0.23. Curve (●) depicts the intermolecular pair correlation function for the beads in the uncollapsed matrix chains. Filler particles and matrix chains are represented by 106 beads.

5. Conclusions

Models for permeable and impermeable filler particles composed of intramolecularly collapsed chains of PE or POE have been characterized. The extent of their collapse is governed by the modification of the intramolecular interaction between pairs of beads when the pair is separated by a distance that produces the strongest attraction in an LJ potential energy function. Complete collapse to dense impermeable particles can be achieved. The collapsed filler particles remain mobile in the amorphous environment formed by uncollapsed matrix chains constructed from the same repeat unit.

The simulation prohibits the energetically driven aggregation of the filler particles. There is no evidence for aggregation of impermeable PE filler particles, even when x_{filler} is as large as 0.60. POE filler particles also avoid aggregation if they are collapsed to a sufficient degree. However, aggregation at intermediate concentration is detected if the filler particles are sufficiently permeable. This aggregation is probably driven by the decrease in conformational entropy of the uncollapsed matrix chains when they must fill the unoccupied space within a permeable filler particle.

Acknowledgements

This research was supported by National Science Foundation grants DMR 0098321 and DMR 0455117.

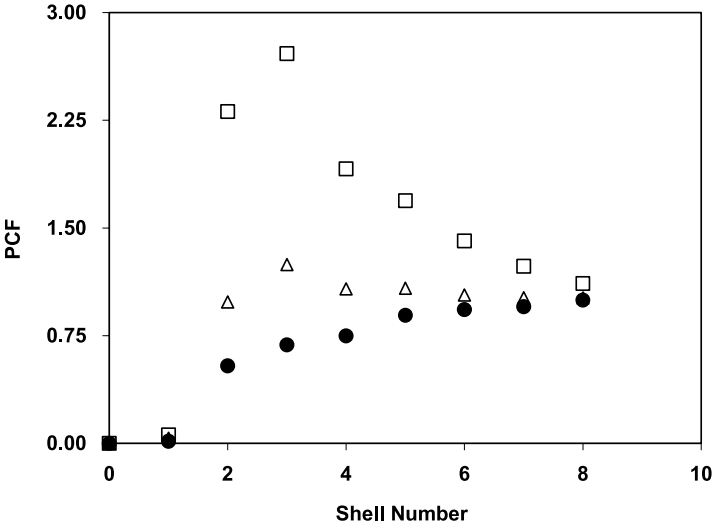

Fig. 10. Intermolecular pair correlation functions for beads in the permeable ($c=0.85\pm0.02$) POE filler particles at 373 K and values of x_{filler} of (●) 0.05, (□) 0.21, and (△) 0.51. Filler particles and matrix chains are represented by 52 beads.

References

[1] Starr FW, Schroder TB, Glotzer SC. Molecular dynamics simulation of a polymer melt with a nanoscopic particle. Macromolecules 2002; 35:4481–92.

[2] Brown D, Mélé P, Marceau S, Albérola ND. A molecular dynamics study of a model nanoparticle embedded in a polymer matrix. Macromolecules 2003;36:1395–406.

[3] Sharaf MA, Kloczkowski A, Mark JE. Simulation on the reinforcement of elastomeric poly(dimethylsiloxane) by filler particles arranged on a cubic lattice. Comput Polym Sci 1994;4:29–39.

[4] Sharaf MA, Mark JE. Monte Carlo simulations on the effects of nanoparticles on chain deformations and reinforcement in amorphous polyethylene networks. Polymer 2004;45:3943–52.

[5] Vacatello M. Chain dimensions in filled polymers: an intriguing problem. Macromolecules 2002;35:8191–3.

[6] Vacatello M. Phantom chain simulations of polymer–nanofiller systems. Macromolecules 2003;36:3411–6.

[7] Park IH, Wang QW, Chu B. Transition of linear polymer dimensions from θ to collapsed regime. Part 1. Polystyrene/cyclohexane system. Macromolecules 1987;20:1965–75.

[8] Park IH, Fetters L, Chu B. Dimensions of ultrahigh molecular weight polystyrene in cyclohexane below the θ temperature. Macromolecules 1988;21:1178–80.

[9] Wu C, Zhou S. Thermodynamically stable globule state of a single poly(*N*-isopropylacrylamide) chain in water. Macromolecules 1995; 28:5388–90.

[10] Wang W, Wu C. Light-scattering study of coil-to-globule transition of poly(*N*-isopropylacrylamide) chain in deuterated water. Macromolecules 1999;32:4299–301.

[11] Kayaman N, Gürel EE, Baysal BM, Karasz FE. Kinetics of the coil-globule collapse in poly(methyl methacrylate) in dilute solutions below Θ temperatures. Macromolecules 1999;32:8399–403.

[12] Maki Y, Sasaki N, Nakata M. Coil-globule transition of poly(methyl methacrylate) in acetonitrile. Macromolecules 2004;37:5703–9.

[13] Williams C, Brochard F, Frisch HL. Polymer collapse. Ann Rev Phys Chem 1981;32:433–51.

[14] Tanaka G, Mattice WL. Chain collapse by lattice simulation. Macromol Theory Simul 1996;6:499–523.

[15] Mackay ME, Dao TT, Tuteja A, Ho DL, Van Horn B, Kim HC, et al. Nanoscale effects leading to non-Einstein-like decrease in viscosity. Nat Mater 2003;2:762–6.

[16] Baschnagel J, Binder K, Doruker P, Gusev AA, Hahn O, Kremer K, et al. Bridging the gap between atomistic and coarse-grained models of polymers. Adv Polym Sci 2000;152:41–156.

[17] Doruker P, Mattice WL. Reverse mapping of coarse grained polyethylene chains from the second nearest neighbor diamond lattice to an atomistic model in continuous space. Macromolecules 1997;30: 5520–6.

[18] Rapold RF, Mattice WL. Introduction of short and long range energies to the simulation of 'real' chains on the 2nnd lattice. Macromolecules 1996;29:2457–66.

[19] Helfer CA, Xu G, Mattice WL, Pugh C. Monte Carlo simulations investigating the threading of cyclic poly(ethylene oxide) by linear chains in the melt. Macromolecules 2003;36:10071–8.

[20] Cho J, Mattice WL. Estimation of long range interaction in coarse-grained rotational isomeric state polyethylene chains on a high coordination lattice. Macromolecules 1997;30:637–44.

[21] Abe A, Jernigan RL, Flory PJ. Conformational energies of *n*-alkanes and the random configuration of higher homologs including polyethylene. J Am Chem Soc 1966;88:631–9.

[22] Abe A, Tasaki K, Mark JE. Rotational isomeric state analysis of poly(oxyethylene). Conformational energies and the random-coil configuration. Polym J 1985;17:883–93.

[23] Haliloglu T, Mattice WL. Mapping of rotational isomeric state chains with asymmetric torsional potential energy functions on a high coordination lattice: application to polypropylene. J Chem Phys 1997; 108:6989–95.

[24] Metropolis N, Rosenbluth AW, Rosenbluth MN, Teller AH, Teller EJ. Equation-of-state calculations by fast computing machines. J Chem Phys 1953;21:1087–92.

[25] Clancy TC, Mattice WL. Rotational isomeric state chains on a high coordination lattice: dynamic Monte Carlo algorithm details. J Chem Phys 2000;112:10049–55.

[26] Clancy TC, Pütz M, Weinhold JD, Curro JG, Mattice WL. Mixing of isotactic and syndiotactic polypropylenes in the melt. Macromolecules 2000;33:9452–63.